World Academy of Science, Engineering and Technology
International Journal of Physical and Mathematical Sciences
Vol:6, No:9, 2012

Numerical Simulation of Convective Heat Transfer and Fluid Flow through Porous Media with DifferentMoving and Heated Walls

Laith Jaafer Habeeb

***Abstract*—**The present study is concerned with the free convective two dimensional flow and heat transfer, within the framework of Boussinesq approximation, in anisotropic fluid filled porous rectangular enclosure subjected to end-to-end temperature difference have been investigated using Lattice Boltzmann method fornon-Darcy flow model. Effects of the moving lid direction (top, bottom, left, and right wall moving in the negative and positive *x*&*y*-directions), number of moving walls (one or two opposite walls), the sliding wall velocity, and four different constant temperatures opposite walls cases (two surfaces are being insulated and the twoother surfaces areimposed to be at constant hot and cold temperature)have been conducted. The results obtained are discussed in terms of the Nusselt number, vectors, contours, and isotherms.

***Keywords*—**Numerical simulation,lid-driven cavity flow,saturated porous medium, different velocity and heated walls.

I. Introduction

FLUID flow and heat transfer in a lid-driven cavity filled with saturated porous medium with buoyancy effect for steady case, have been an important topic because of its wide application area in engineering and sciencevarying from environmentalapplications to inkjet printing technology. Some of these applications include heat exchangers, flow and heat transfer in solar power collectors, packed-bed catalytic reactors, nuclear energy systems,cooling of electronic systems, chemical processing equipment, lubricating grooves, coating and industrial processes,metal casting,galvanizing and metal coating, float glass manufacturing,dynamics of lakes and large reservoirs, crystal growth, food processing and so on.Numerous investigations have been conducted in the past on lid-driven cavity flow and heat transfer considering various combinations of the imposed temperature gradients and cavity configurations. Such configurations can be idealized by the simple rectangular geometry with regular boundary conditions yielding a well-posed problem. The resulting flow however, is rather complex even when the flow is purely shear driven for the isothermal case without any temperature gradient. When a temperature gradient is imposed such that the shear driven andbuoyancy effects are of comparable magnitude then the resulting flow falls under the convection regime and the interaction and coupling of these effects makes the analysis more complex.

Laith J. Habeeb is with the Mechanical Engineering Dept.,University of Technology,Baghdad – Iraq(e-mail: laithjaafer@yahoo.com , or, dr.laith_jaafer@uotechnology.edu.iq).

In general, the current numerical models to predictthe flow through porous media fall in four categories: The Darcy model, the Forcheimer model, the Brinkman model and the Brinkman-Forcheimer model. The Darcymodel was developed based on the original Darcyequation. However, this model is reported to produceunsatisfactory results when compared with the theoretical prediction based on Darcy law. In Forcheimer model, it considers the non-linear drag effect due to the solid matrix while the Brinkman model includes the viscous stress introduced by the solidboundary. Even though these two models have been widely used by many researchers, they are not general enough to be applicable for a medium with variable porosity. In recent years, the Lattice Boltzmann Method (LBM) has received considerable attention as an alternative approach for simulating wide range of fluid flow. Unlike other numerical methods, LBM predicts the evolution of particle distribution function and calculates the macroscopic variables by taking moment to the distribution function. The LBM has a number of advantages over other conventional computational fluid dynamics approaches. The algorithm can also be easily modified to allow for the application of other, more complex simulation components. Ekkehard[1]was outlined an increasingly more complex situationsdescribed as(a)advection-diffusion,(b)free convection, (c)forced convection and (d)mixed convection for simple systems in porous media exemplifying steady state solutions. Hakan[2] perform a numerical work to analyze combined convection heat transfer and fluid flow in a partially heated porous lid-driven enclosure.

The top wall of enclosure moves from left to right with constant velocity and temperature. Heater with finite length is located on the fixed wall where its center of location changes along the walls. The finite volume-based finite-difference method is applied for numerical experiments. Parameters effective on flow and thermal fields are Richardson number, Darcy number, center of heater and heater length. The results were shown that the best heat transfer is formed when the heater is located on the left vertical wall.WatitandPhadungsak[3] studiedthe transient natural convection flow through a fluid-saturated porous medium in a square enclosure with a convection surface condition. The cavity was insulated except the top wall that was partially exposed to an outside ambient. The exposed surface allows convective transport through the porous medium, generating a thermal stratification and flow circulations. The finite difference equations handling the convection boundary condition of the open top surface are derived for heating and cooling conditions.

A lateral temperature gradient in the region close to the top wall induces the buoyancy force under an unstable condition. The directions of vortex rotation generated under the two different conditions were opposite. It was found that the heat transfer coefficient, Rayleigh number and Darcy number considerably influenced characteristics of flow and heat transfer mechanisms. Sharif[4] studied numericallythe laminar mixed convective heat transfer in two-dimensional shallow rectangular driven cavities of aspect ratio 10. The top moving lid of the cavity was at a higher temperature than the bottom wall. The fluid Prandtl number was taken as 6 representing water. The effects of inclination of the cavity on the flow and thermal fields were investigated for inclination angles ranging from 0^o to 30^o. Interesting behaviors of the flow and thermal fields with increasing inclination were observed. The average Nusselt number was found to increase with cavity inclination. The rate of increase of the average Nusselt number with cavity inclination was mild for dominating forced convection case while it was much steeper in dominating natural convection case.Wang [5] investigate the lid-driven rectangular cavity containing a porous Darcy–Brinkman medium. The governing equation was solved by an eigenfunction method which is much simpler than using biorthogonal series. It was found that the porous medium effect decreases both the strength and the number of recirculating eddies, especially for deep cavities.Mohd*et al* [6] investigate fluid flow behavior through porous media in a lid-driven square cavity.The Brinkman-Forcheimer equation was coupled with the lattice Boltzmann formulation to predict the velocity field in the system. Three numerical experiments were performed with different values of Darcy number to investigate the effect of porosity on the fluid flow. Theyfound that the magnitude of velocity, strength of vortex and velocity boundary layer is significantly affected porosity of the media.The lattice Boltzmann simulation scheme is capable in prediction of fluid flow behavior through porous media.Mohamed and Wael [7]concerned with the mixed convection in a rectangular lid-driven cavity under the combined buoyancy effects of thermal and mass diffusion. Double-diffusive convective flow in a rectangular enclosure with moving upper surface is studied numerically. Both upper and lower surfaces are being insulated and impermeable. Constant different temperatures and concentration are imposed along the vertical walls of the enclosure. The numerical results are reported for the effect of Richardson number, Lewis number, and buoyancy ratio on the iso-contours of stream line, temperature, and concentration. In addition, the predicted results for both local and average Nusselt and Sherwood numbers are presented and discussed for various parametric conditions. MOHD [8] applied (LBM) to predict the phenomenon of natural convection in a generalized isotropic porous media model filled in a square geometry by introducing a force term to the evolution equation and porosity to the density equilibrium distribution function. The temperature field was obtained by simulating a simplified thermal model which useslessvelocity directions for the equilibrium distribution function and neglects the compression work done by the pressure and the viscous heat dissipation. The model was used for simulation at ε equal to 0.4, 0.6 and 0.9. The results obtained were discussed in terms of the Nusselt number, streamlines and isotherms.

Comparison with previous works confirms the applicability of the model. Safaiy and Goshayeshi [9] modeled the laminar mixed convection inside rectangular enclosure with moving wall and Aspect Ratio=10 and then the results were compared with other investigate. After showing variety of results, the investigation was continued with turbulent flow using RNG $\varepsilon-k$ and standard $\varepsilon-k$. The results indicated that the turbulence intensity depends on the position. Waheed*et al* [10]investigate numerically the mixed convective heat transfer in a fluid-saturated porous medium using the generalized non-Darcy model. The flow governing parameters including the Darcy, Richardson and Péclet numbers, and the length-to-height aspect ratio were varied in the range $10^{-3} \leq Da \leq 10$, $0.1 \leq Ri \leq 10$, $1 \leq Pe \leq 10^3$and $0.5 \leq AR \leq 4$ respectively while the Reynolds number was held constant at a value of $Re = 100$ for all computations. The results show that all the flow governing parameters have strong influence on the flow pattern and heat distribution within the enclosure.Prakashand Satyamurty [11] investigate the free convective flow and heat transfer, in an anisotropic fluid filled porous rectangular enclosure using Brinkman extended non-Darcy flow model. The studies involve simultaneous consideration of hydrodynamic and thermal anisotropy. Numerical solutions employing the successive accelerated replacement (SAR) scheme have been obtained for $100 \leq Ra \leq 1000$,$0.5 \leq AR \leq 5$,$0.5 \leq K^* \leq 5$,$0.5 \leq k^* \leq 5$, and $0 \leq Da \leq 0.1$. It has been found that average Nusselt number increases with increase in $K^*$and decreases as $k*$increases. However, the magnitude of the change in average Nusselt number depends on the parameter *Da*, characterizing the Brinkman extended non-Darcy flow.Ilyas and Alaattin [12] conductedhard-sphere molecular dynamics simulations of lid-driven microcavity gas flow with various subsonic speeds and lid temperatures. Simulations with faster and colder lids show streamlines of stronger primary vortices. Center of energy was less sensitive to employed lid conditions than center of gravity is. Although moving lid imparts energy into fluid, due to change of impingement rates on the walls of fixed temperature, average energy within the cavity seems quite insensitive to the subsonic lid speed. While high Knudsen number causes considerable property slips near the lid, two-dimensional pressure, density, and temperature plots of excellent quality are generated. Khaled*et al* [13] analyzedeffects of moving lid-direction on MHD mixed convection in a cavity with the bottom wall being linearly heated using a numerical technique. Vertical walls of the enclosure were adiabatic and the sliding wall at the top has constant temperature. The lid moves in the negative and positive x-direction. Finite volume method has been used to solve the governing equations. Results werepresented for different values of Hartmann number ($0 \leq Ha \leq 30$), Reynolds number ($100 \leq Re \leq 1000$) and Grashof number ($10^4 \leq Gr \leq 10^6$). It was found that direction of lid is more effective on heat transfer and fluid flow in the case of mixed convection than it is the case in forced convection. Heat transfer is also decreased with increasing of magnetic field for all studied parameters.

From the previous review it is denoted that the recent researches in moving lid direction and velocity in porous media with different heated wall is very limited.

So, my concern in this study is to study the effects of moving one or two of the cavity walls, the sliding wall direction andvelocity, and the best heating side direction of the opposite walls.

II. The Physical And Mathematical Models

A. Problem description

A schematic of the system and all cases considered in the present study is shown in Fig. (1). The system consists of a square enclosure with sides of length H, filled with a fluidsaturated porous mediumand Prandlt number (*Pr*) =1.0. The problem has been studied assuming that: the gravitational acceleration acts in the negative *y*-direction, Rayleigh number (*Ra*)=1000, porosity (ε)=0.7, and Darcy number (*Da*)=0.01. As the square enclosure are long enough, so the flow is consider to betwo dimensional,the fluid and the solid matrix are in thermal equilibrium, and the porous medium is homogeneous.This study will be limited to: steady state incompressible fluid flow, square enclosure with differentially heated walls, isotropic porous media, and non-Darcy region.

The numbers of all cases considered in this study are 25 different physical domains. Always twoof the opposite walls are subjected to hot and cold temperatures, and the other twowalls are insulated. The moving lid or walls is considered in 21 cases when the temperatures $T_h$and $T_c$are uniformly imposed along the vertical left and right walls respectively. The top and bottom surfaces are assumed to be adiabatic.

In cases (1-8) only one surface is moving at 0.2 m/s, as follows respectively: the lower wall to the left (-*x* direction) and to the right (+*x* direction), the left wall to down (-*y* direction) and to up (+*y* direction), the right wall to down and to up, and the upper one to the left and to the right.

In cases (9-16) two surfaces are moving at 0.2 m/s, as follows respectively: the left and the right walls move in -*y* direction, the left wall moves in -*y* directionand the right wall move in +*y* direction, the upper and lower walls move in -*x* direction, the upper wall to the left and lower one move in +*x* direction, the upper wall moves in +x directionand lower one moves in -*x* direction,the upper and lower walls move in +*x* direction, the left wall moves in +*y* directionand the right wall moves in -*y* direction, and the left and the right walls move in +*y* direction.

In cases (17-21) only the lower surface is moving in +*x* directionat 0.1 m/s, 0.15 m/s,0.25 m/s,0.3 m/s,and 0.4 m/s respectively.

In cases (22-25) stationary walls are considered but with different hot and cold opposite walls locations. In case (22) the hot vertical wall is to the left and coldone is to the right. The top and bottom surfaces are assumed to be adiabatic. In case (23) the cold vertical wall is to the left and hotone is to the right. Also, the top and bottom surfaces are assumed to be insulated. In case (24) the hot horizontal wall is the upper surface and coldone is to thelower surface. The left and right surfaces are assumed to be adiabatic. In case (25) the cold horizontal wall is the upper surface and hotone is to thelower surface. Also, the left and right surfaces are assumed to be adiabatic.

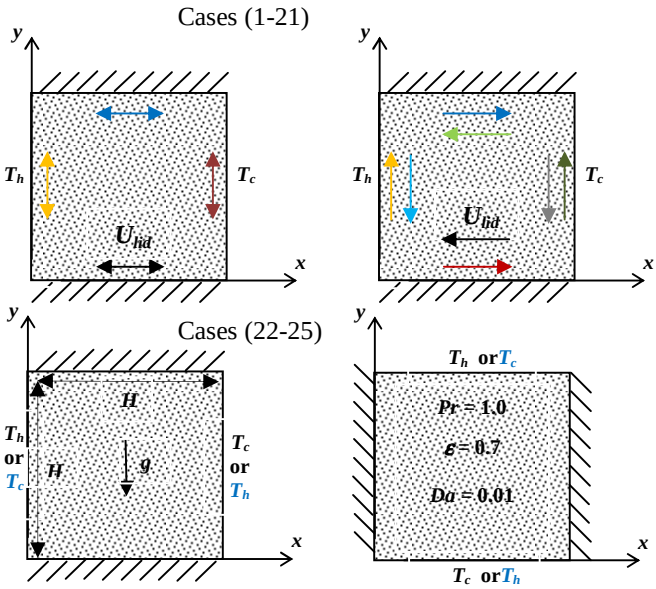

Fig. 1 Schematic diagram for the problem,physical models and caseswith the wall boundary constraints and the coordinate axes.

B. Governing Equations

Following [6] and [8], the generalized model for incompressible fluid flow through porous media can be expressed by the following equations:

$$\nabla \cdot u = 0 \tag{1}$$

$$\partial u/\partial t + (u \cdot \nabla)(u/\varepsilon) = -(1/\rho)\nabla(\varepsilon\, p) + \upsilon_\varepsilon \nabla^2 u + F \tag{2}$$

F represents the total body force due to the presence of porous media and is given by:

$$F = -(\varepsilon \upsilon / K)\, u - \left(1.75/\sqrt{150\,\varepsilon K}\right)|u|\, u + \varepsilon\, G \tag{3}$$

The permeability (K) of which can be related to no dimensional parameter of Darcy number *Da* as follow:

$$K = Da \times H^2 \tag{4}$$

In the formulation of LBM, the starting point is the evolution equation, discrete in space and time, for a set of distribution functions *f*. If a two-dimensional nine-velocity model (D2Q9) is used for flow field and two-dimensional four-speed (D2Q4) Lattice Boltzmann equation(LBE)model is used to simulate the temperature field, then the evolution equations for a given *f*and *g* takes the following forms:

$$\begin{aligned} &f_i(x + e_i \Delta t, t + \Delta t) - f_i(x,t) = \\ &\quad -1/\tau_f \left[f_i(x,t) - f_i^{eq}(x,t)\right] + F_i \end{aligned} \tag{5}$$

$$\begin{aligned} &g_i(x + e_i \Delta t, t + \Delta t) - g_i(x,t) = \\ &\quad -1/\tau_g \left[g_i(x,t) - g_i^{eq}(x,t)\right] \end{aligned} \tag{6}$$

Where i = 0,1,…,8 for f and i = 1,2,3,4 for g.

Where distribution function$f_i$is used to calculate density and velocity fields while distribution function is used to g_i to calculate temperature field. Here, e denotes the discrete velocity set and expressed as:

$$e_i = \begin{cases} (0,0), & i = 0 \\ (\pm 1,0),(0,\pm 1), & i = 1 - 4 \\ (\pm 1,\pm 1), & i = 5 - 8 \end{cases} \quad (7)$$

f_i^{eq},$g_i^{eq}$are equilibrium distribution functions, the choice of which determines the physics inherent in the simulation. For D2Q9 and (D2Q4) models, $f_i^{eq}$and$g_i^{eq}$are expressed as:

$$f_i^{eq} = \rho\omega_i\left[1 + 3e_i \cdot u + (9/2)\left((e_i \cdot u)^2/\varepsilon\right) - (3/2)\left((u)^2/\varepsilon\right)\right] \quad (8)$$

$$g_{1,2,3,4}^{eq} = \rho T(1/4)\left[1 + \left(e_i \cdot u / c^2\right)\right] \quad (9)$$

Where, the weights areω_0= 4/9,$\omega_{1\text{-}4}$= 1/9 and $\omega_{5\text{-}8}$= 1/36. The time relaxation and the effective viscosity can be related as follow:

$$\upsilon_\varepsilon = (1/3)(\tau - (1/2)) \quad (10)$$

In order to obtain the correct macroscopic governing equations, the forcing term $F_i$must be expressed in terms of medium porosity as follow:

$$F_i = \rho\omega_i(1 - (1/2\tau))\cdot \left[3e_i \cdot F + \left(9(uF : e_i e_i)^2/\varepsilon\right) - (3u \cdot F/\varepsilon)\right] \quad (11)$$

The macroscopic density and the macroscopic flow velocity can then be calculated as follow:

$$\rho = \sum_{i=1}^{9} f_i^{eq} \quad (12)$$

$$v = \sum_i e_i f_i / \rho + (\varepsilon G/2) \quad (13)$$

and:

$$u = v/\left(c_0 + \sqrt{c_0^2 + c_1|v|}\right) \quad (14)$$

where:

$$c_0 = (1 + \varepsilon\upsilon/2K)/2 \quad and \quad c_1 = 1.75\varepsilon/2\sqrt{150\varepsilon^2 K}$$

It is noted that, if we set ε= 1, the Lattice Boltzmann equation reduces to the standard equation of free fluid flows.

Boussinesq approximation is applied to the buoyancy force term. With this approximation, it is assumed that all fluid properties are constant except for density change with temperature.

$$G = \beta g(T - T_m)j \quad (15)$$

The dynamical similarity depends on three dimensionless parameters: the Prandtl number (*Pr*), Rayleigh number (Ra) and Nusselt number (*Nu*).

$$Pr = \upsilon/\chi \quad (16)$$

$$Ra = \rho\beta(T_h - T_c)L^3/\upsilon\chi \quad (17)$$

$$Nu = (H/\chi\Delta T)\left(1/H^2\right)\int_0^H\int_0^H q_x(x,y)dx\,dy \quad (18)$$

Where: $q_x(x,y) = uT - \chi(\partial/\partial x)T(x,y)$is the local heat flux in *x*-direction.

III. Numerical Simulation

The present algorithmused is the same in [8], itbegin with main program with seven subroutines. The program is modified to fulfill the required different present cases and to handlemore complex geometries. The numerical data obtained for each node are used to plot graphical representation of vectors, contours and isotherms.Simulations were done by programming which uses Fortran PowerStation 4.0 (Microsoft Developer Studio). Desktop PC with Intel (R) Core(TM)2 Quad CPU, 3GHz processor and 4.00 GB RAM was used to run the simulation.

Numerical stability and iteration to converge need the particles to be at equilibrium state. This will be obtained by manipulating the value of the time relaxation. The value of time relaxation needs to be closer to 1. The closer time relaxation to 1, the more number of particles will be exchanged to equilibrium state. The main iteration is repeated until a convergence solution is obtained at convergence criteria for the velocity less than 1×10^{-8}. In the simulations, mesh sizes (101×101), (151×151) and (201×201) were used for Rayleigh Numbers = 10^3, 10^4 and 10^5 respectively.

The calculations of average Nusselt numbers for the present program are compared early by [8]with other single phase fluid resultsfor different values of Rayleigh number as given in table (1). In this comparison, the porosity (ε) is set to 0.9999, the Darcy number = 10^7 and Prandtl number = 0.72. When the porosity approaches unity and the Darcy number is relatively large, the Brinkman-Forchheimer equation reduces to Navier-Stokes equation for free fluid flows. In table (1), the average Nusselt number obtained is compared with those of the benchmark results by [14], [15],[16] and [8].

The comparison showed that the obtained Nusselt number is acceptable. The simulation has successfully resembled a free fluid flow. However, the Nusselt number of the present study is underestimated for Ra = 10^5 and higher because the grid size chosen does not give enough magnitude of characteristic length H. It is expected that a more accurate result can be produced if larger grid sizes are used [8].

TABLE I
Comparison of average Nusselt number with other single phase fluid results

Ra	[14]	[15]	[16]	Present
10^3	1.116	1.127	1.117	1.117
10^4	2.238	2.245	2.244	2.236

Next, applicability of the present Lattice Boltzmann model for simulation of Brinkman-Forchheimer equation is verified. In this second comparison (also earlydone by [8]), the porosity(ε) is set to 0.9, 0.6 and 0.4, Darcy number = $10^{-2}$and Prandtl number = 1.0.

In table (2), the average Nusselt number obtained is compared with those of [15], and [16]. The comparison with previous studies showed that the Nusselt number obtained is also acceptable.

TABLE II
COMPARISON OF AVERAGE NUSSELT NUMBER WITH OTHER RESULTS FOR PR = 1.0 AND DA = 10^{-2}

$Ra = 10^3$	$\varepsilon = 0.9$	$\varepsilon = 0.6$	$\varepsilon = 0.4$
[15]	1.023	1.015	1.01
[16]	1.017	1.012	1.007
Present program	1.019	1.012	1.08
$Ra = 10^4$	$\varepsilon = 0.9$	$\varepsilon = 0.6$	$\varepsilon = 0.4$
[15]	1.64	1.530	1.408
[16]	1.633	1.493	1.362
Present program	1.721	1.495	1.313
$Ra = 10^5$	$\varepsilon = 0.9$	$\varepsilon = 0.6$	$\varepsilon = 0.4$
[15]	3.91	3.555	2.983
[16]	3.902	3.433	2.992
Present program	3.635	3.437	2.982

IV. RESULTS AND DISCUSSION

The results are presented for a number of cases (25 different physical domains) corresponding to *sixteen*movement cases, moreover to *five* cases for lid velocity range $0.1 \leq U_{lid} \leq 0.4$ and *four*different heated opposite walls cases. The basic features of flow and heat transfer are analyzed with the help of the vectors, contour patterns and isothermal contours.Also, average Nusselt numbers for all cases are tabulatedand velocity components are plotted.Some of the results (that I find research to compare with) have the same behavior of the approximatelysimilar published cases. Heat transfer in low speed lid-driven cavity flow is treated mostly as mixed convection. The flow driven by the movement of one or two of the walls is creating a forced convection conditions while temperature difference across the cavity causes a buoyancy driven, secondary flow. Thus, complicated patterns of heat and mass transfer occur inside the cavity.

A. Movement direction effect

Fig.(2)showsthe velocity vectorsand temperature contours for the lid-driven square cavity filled with porous medium for one side movement.Fig. (2-A) shows the velocity vectors with *y*-component velocity contours for case (1). When the lower wall moves to the left, a big clockwise vortex is generated in the whole domain and a small clockwise two vortices is generated near the left wall. Two contours are appeared, the first refers to downward velocity at the right corner with minimum magnitude at the beginning of the moving wall and the second refers to upward velocity at the left corner with maximum magnitude at the end of the moving wall.

Fig. (2-B) shows the temperature contours for case (1). The moving lid transfers the heat from the left side and the big vortex caries the heat to the center as shown at the upper wall.Fig. (2-C) shows the velocity vectors with *y*-component velocity contours for case (2). When the lower wall moves to the right, a big counterclockwise vortex is generated in the whole domain and a small counterclockwise two vortices is generated near the left wall. Two contours are appeared, the first refers to downward velocity at the left corner with minimum magnitude at the end of the moving wall and the second refers to upward velocity at the right corner with maximum magnitude at the beginning of the moving wall. Fig. (2-D) shows the temperature contours for case (2). The moving lid concentrates the heat at the left side and the big vortex caries some of the heat to the center as shown at the lower wall.Fig. (2-E) shows the velocity vectors with *x*-component velocity contours for case (3). When the hot left wall is moving to downward, the*x*-component velocity maximized in the upper left corner because it works as a suction region. The temperature distribution (not shown here) minimizes the thermal boundary layer and the case considered a bad choice. Fig. (2-F) shows the velocity vectors with *x*-component velocity contours for case (4).When the hot left wall is moving to upward, the *x*-component velocity maximized in the upper left corner too but the big vortex is modifyingthe heat transfer. Fig. (2-G)and (2-H) show the velocity vectors with *x*-component velocity contours for cases (5 and 6) respectively.Also, vortices are formed and the velocity is concentrated at the upper and lower corners of the right wall. Case (6) is considered a bad choice too.

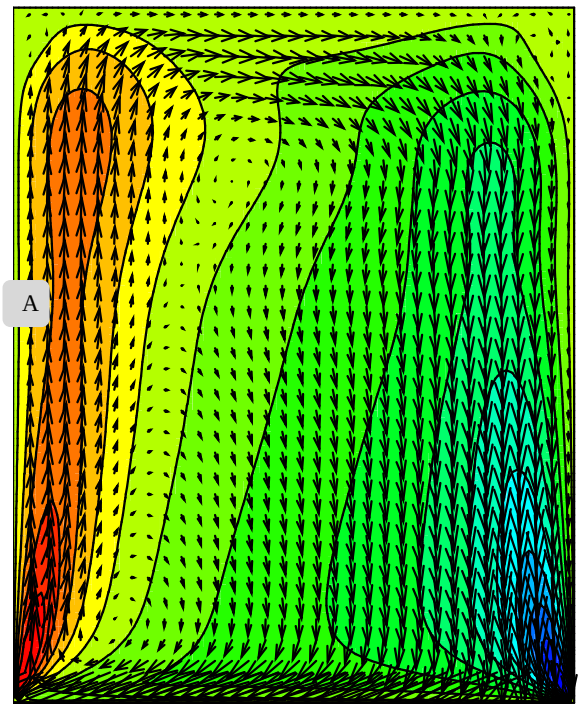

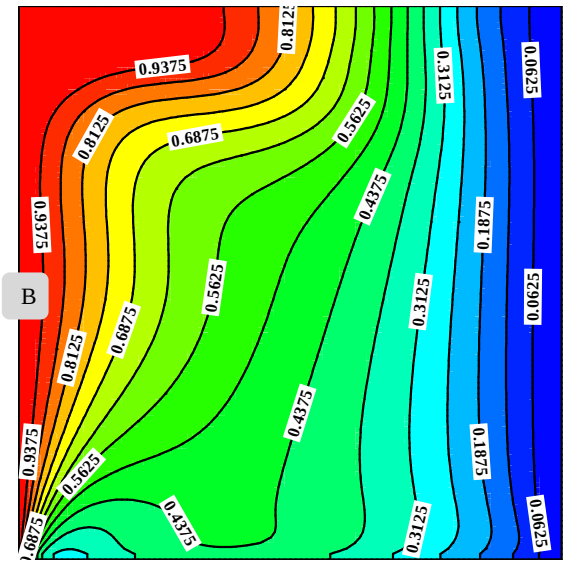

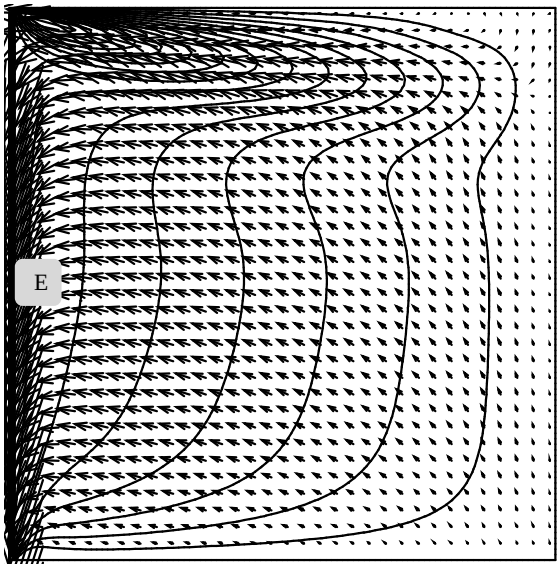

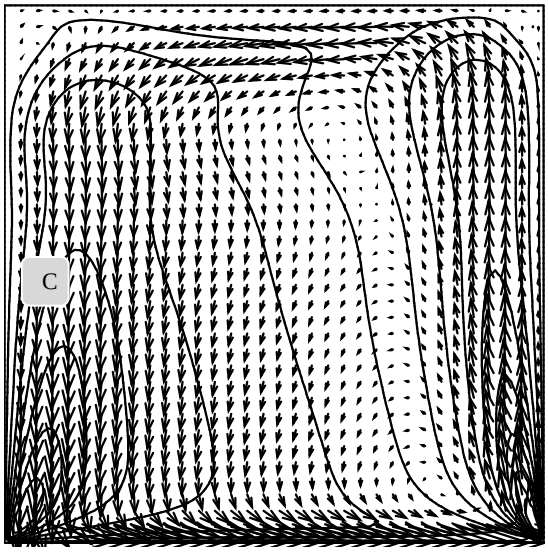

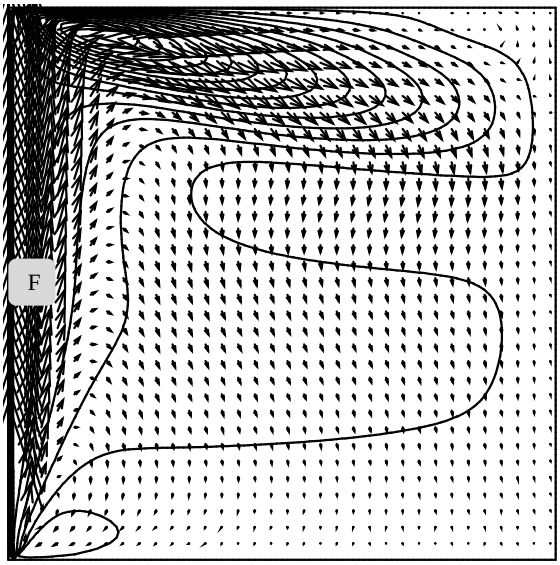

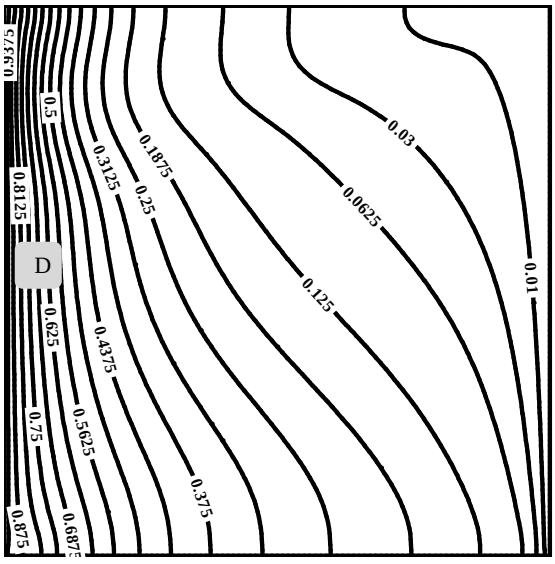

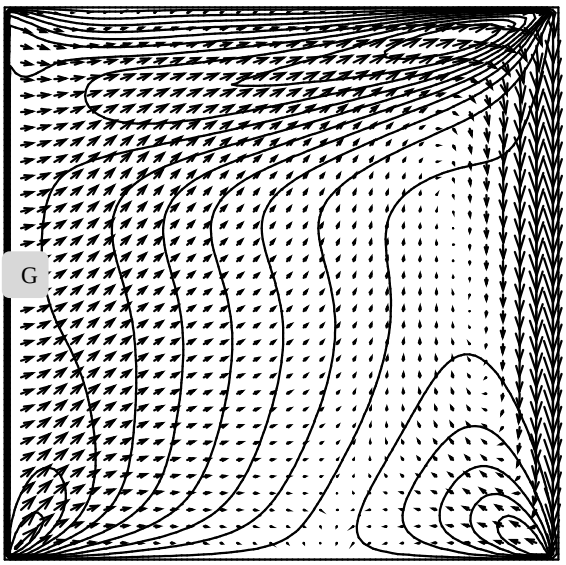

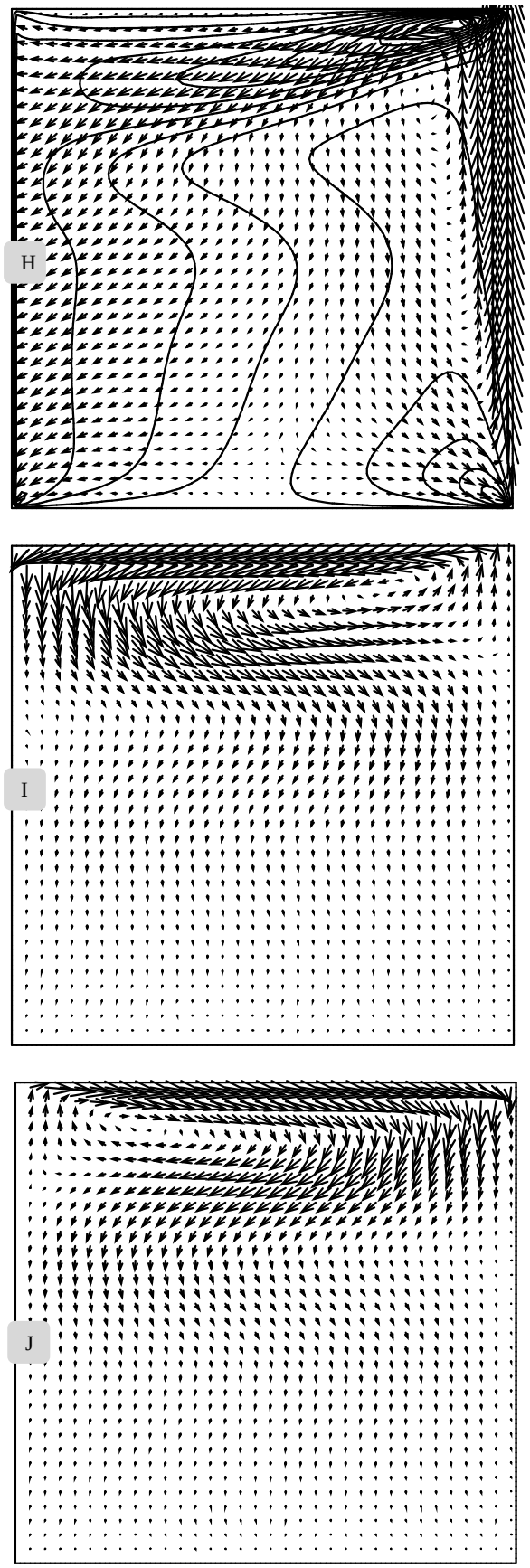

Fig. 2 Velocity vectors, contours and temperature contours forcases (1-8)

Fig. (2-I) and (2-J) show the velocity vectors for cases (7 and 8) respectively. A wavy motion is generated with small vortex. The thermal boundary layer (not shown here) depicts heat transfer improvement.

Fig. 3 shows the velocity distributions (*x*-component) along the box height and (*y*-component) along the box width. Fig.(3-A) shows the velocity distributions (*x*-component) along the box height for cases (1, 2, 7, and 8).A symmetric behavior is noticed with maximum velocity near the moving wall and minimum velocity near the opposite wall. Fig. (3-B) shows the velocity distributions (*y*-component) along the box width for cases (1, 2, 7, and 8). Again a symmetric behavior is noticed but a better heat transferaugmentation occurs when the lower wall is moving to the left or to the right than the upper wall movement, because a better velocity distribution is occurred.

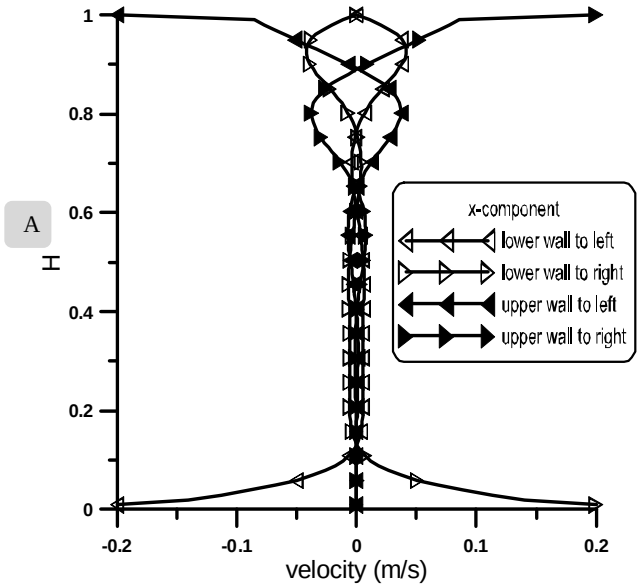

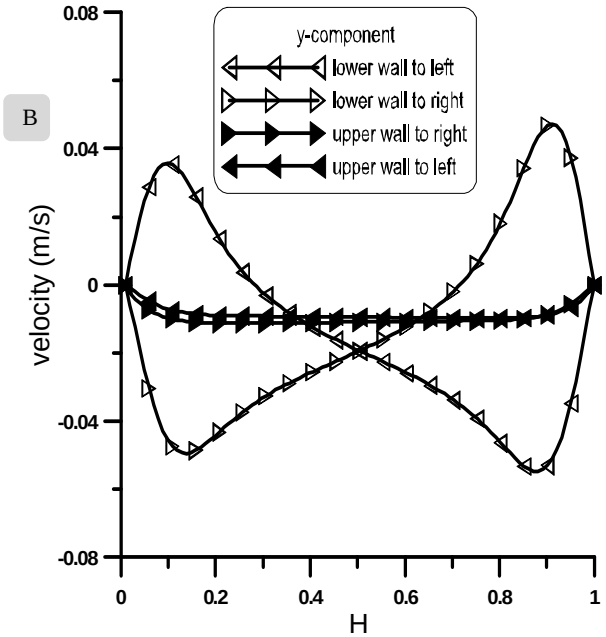

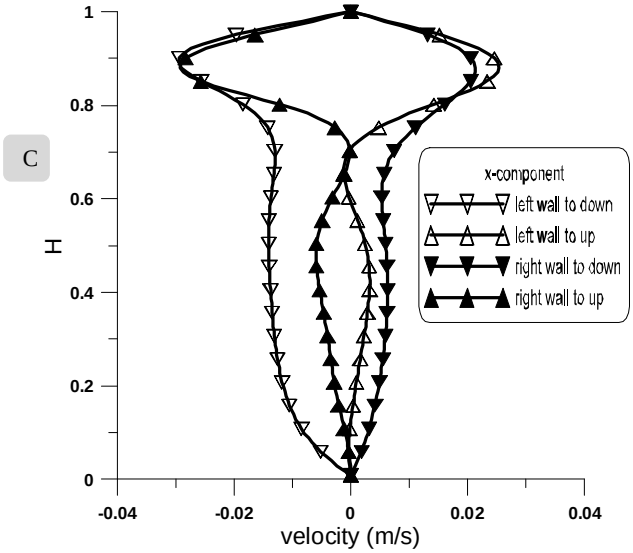

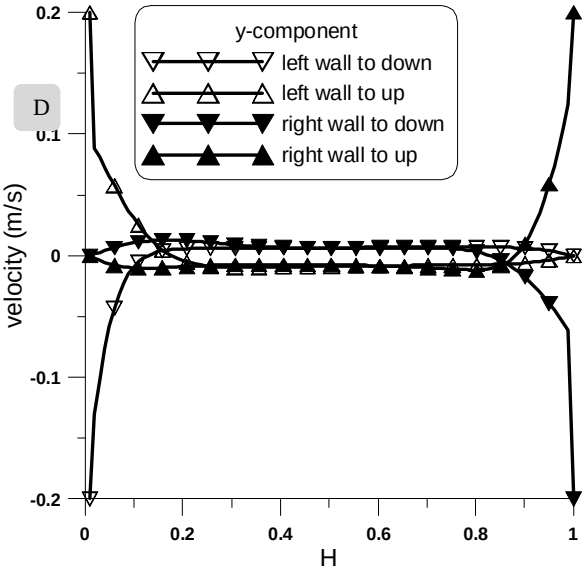

Fig. 3Velocitiesdistributions forcases (1-8)

Fig. (3-C) shows the velocity distributions (*x*-component) along the box height for cases (3, 4, 5, and 6).Cases (3 and 6) cause a negative velocity in the *x*-direction which means bad heat carrying from the heated wall to the opposite cold wall (positive*x*-direction). Fig. (3-B) shows the velocity distributions (*y*-component) along the box width for cases (3, 4, 5, and 6). Cases (4 and 5) are good choice to heat transfer augmentation.

Fig. 4 shows the velocity vectors and temperature contoursfor two sided movement.Fig. (4-A, B, and C) shows thevelocity vectors for case (9, 10, and 11) respectively.Two symmetric vortices are noticed in case (9). Two small vortices near the left wall are noticed in case (11) which causes big thermal boundary layer as shown in Fig. (4-D). This behavior is repeated approximately for cases (12 and 13) in fig.(4-E, F and G) respectively.

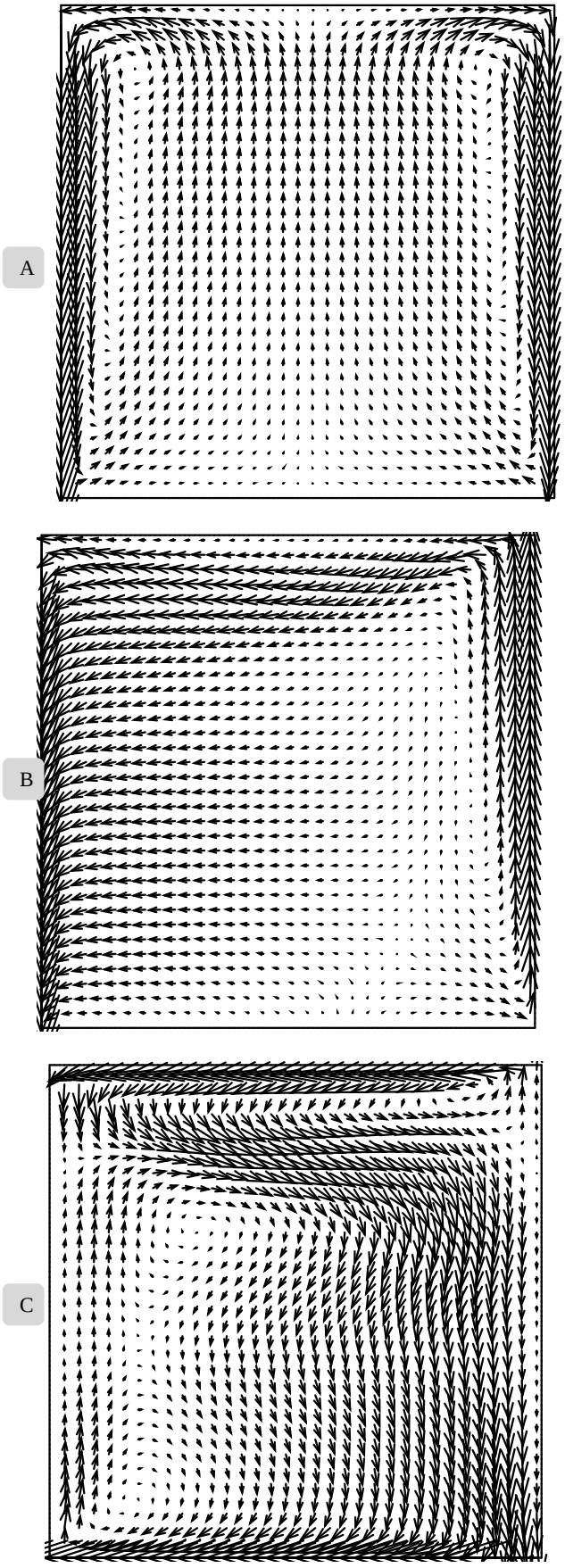

D

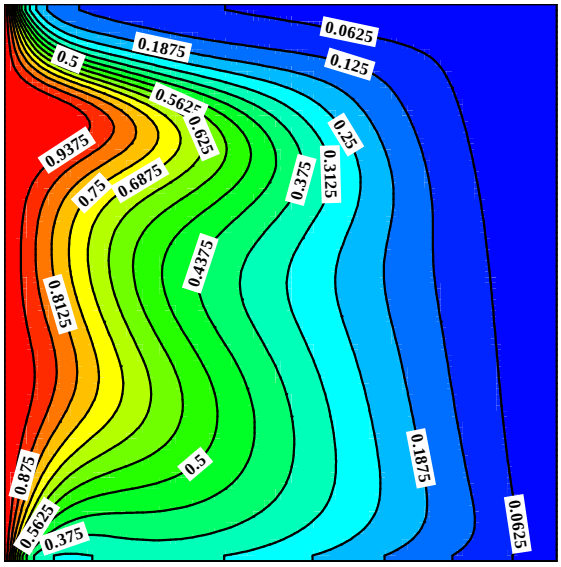

G

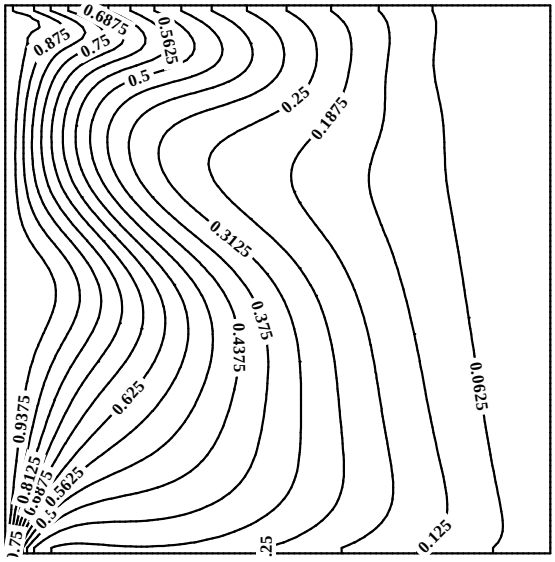

E

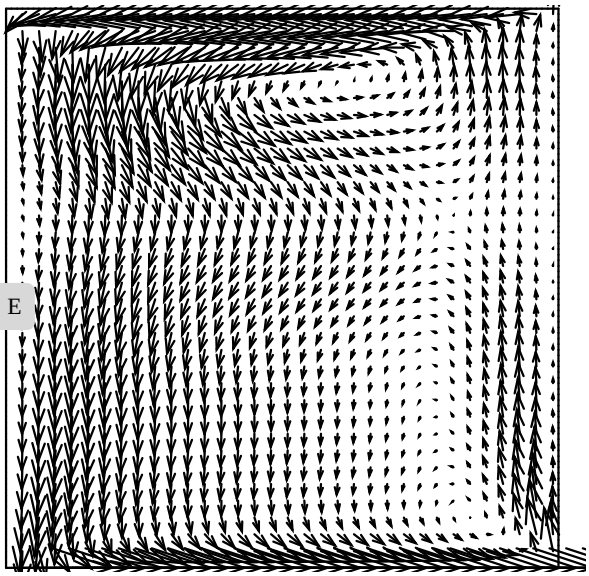

H

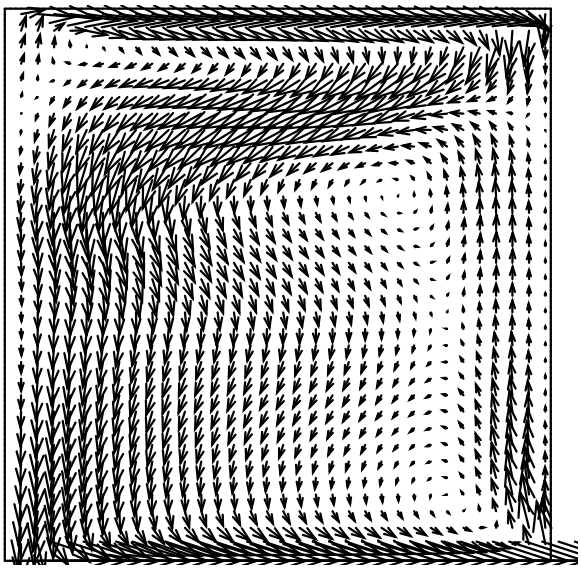

F

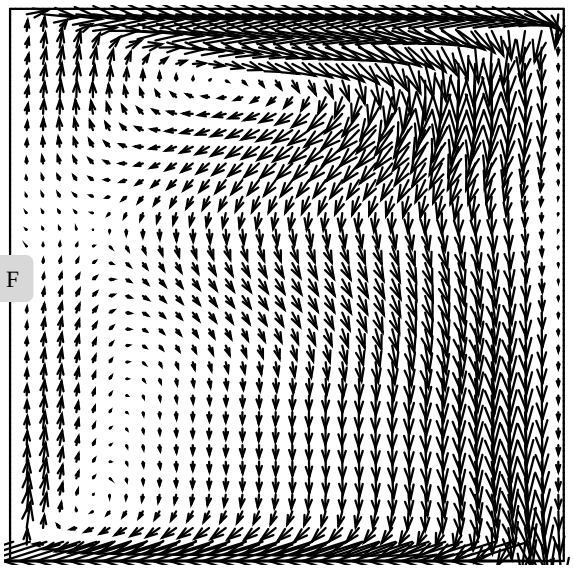

I

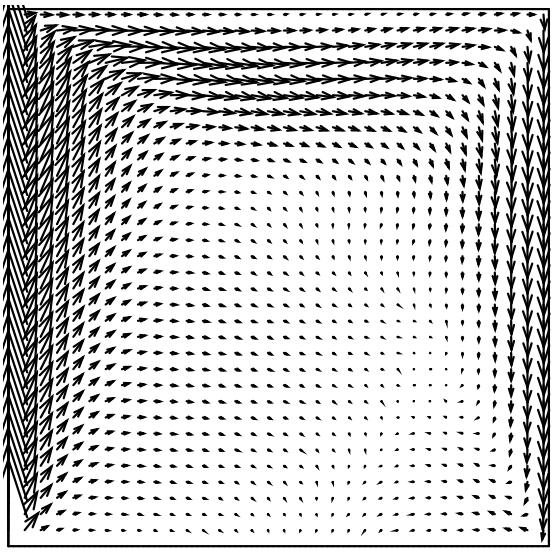

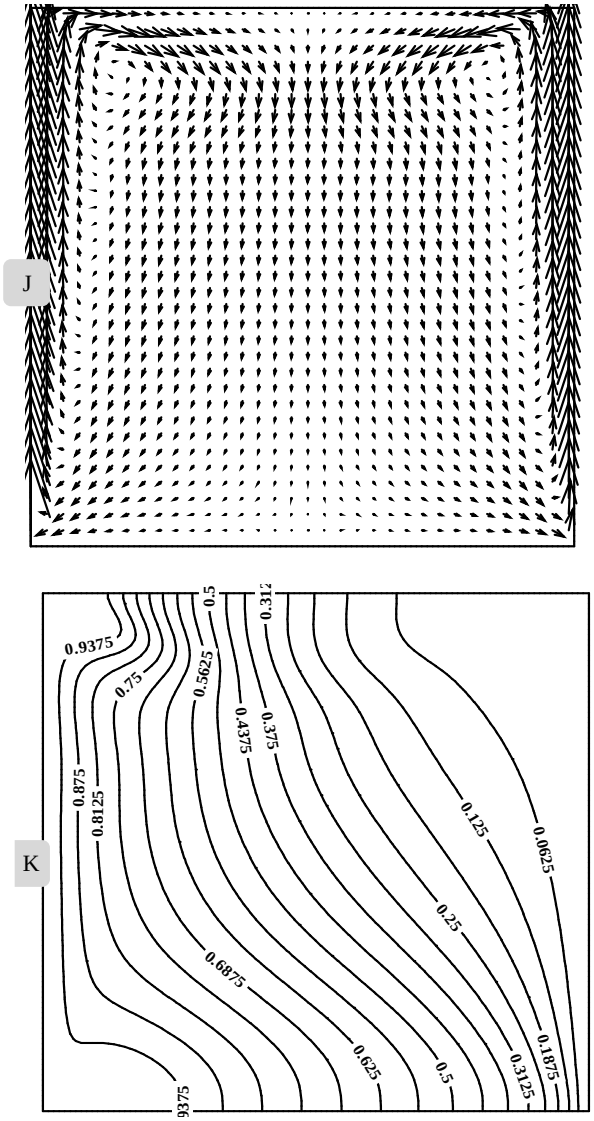

Fig. 4Velocity vectors, contours and temperature contours forcases (9-16).

Fig. (4-H, I, and J) show the velocity vectors for cases (14, 15, and 16). The same behaviors with opposite vortices direction are observed.Fig. (4-K) shows the temperature contours for case (16). The left vortex carry the heat to the center of the box and the right vortex dissipate it to the right part of the box.

Fig. 5 shows the velocities distributions (*x*-component) along the box height and (*y*-component) along the box width for cases (9-16). Fig.(5-A and B) show the velocities distributions (*x* and *y*-components) for cases (9, 10, 15, and 16). Cases (10 and16)are decreases the heats transfer especially case (10) because of the velocity component deformation. Fig. (5-C and D) show the velocities distributions (*x* and *y*-components) for cases (11, 12, 13, and 14).These good symmetric distributions cause big thermal boundary layers that cause heat transfer augmentation.

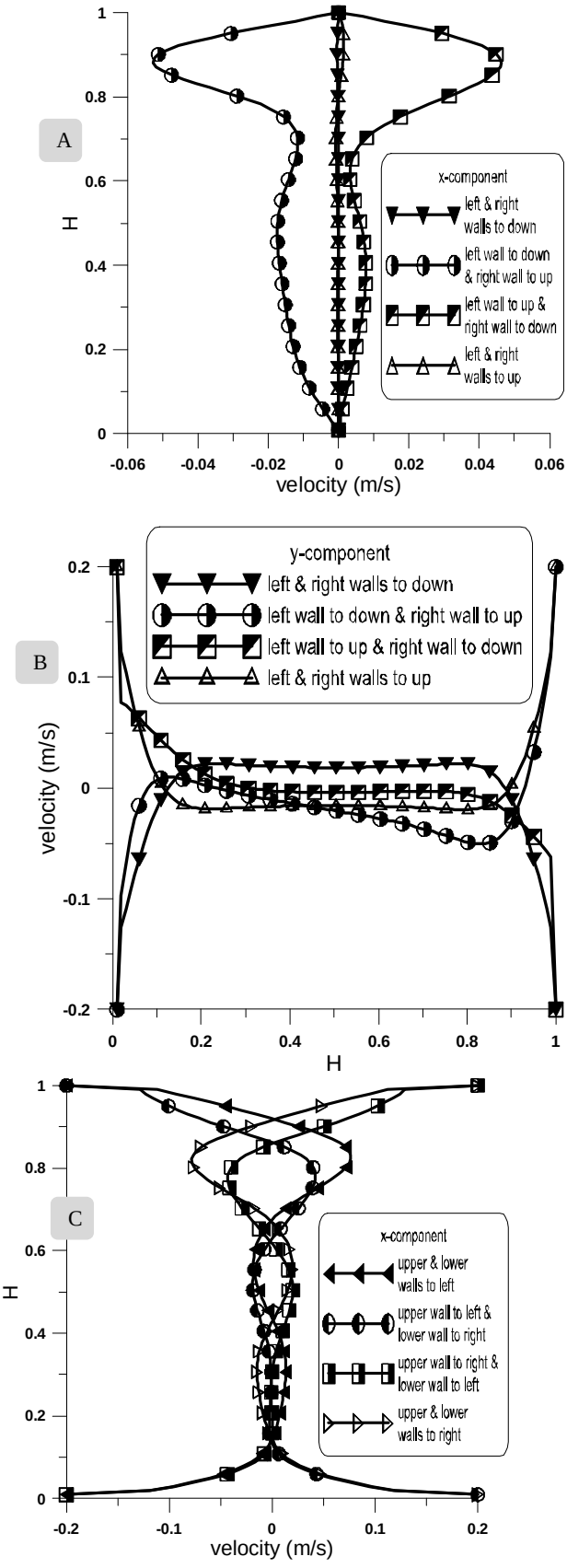

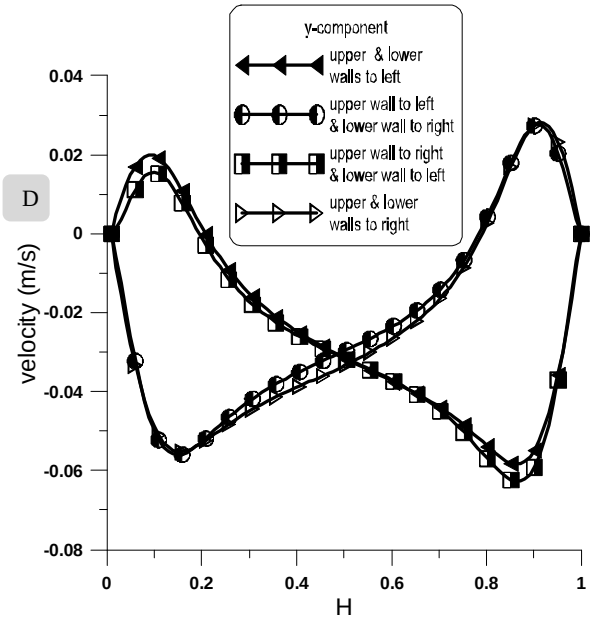

Fig. 5Velocitiesdistributions forcases (9-16)

B. Sliding velocity magnitude effect

Fig. 6 shows the velocities distributions (*x*-component (6-A)) and (*y*-component(6-B)) for cases (17-21).The same behavior of case (2) is mentioned here and the differences are only in magnitudes. As the lid velocity increases, either no influence observed in the axial velocity component in upper layers or the vertical velocity component increases downward. The *x*-component in upper layer do not change when the lower wall moves to the right and only the near wall layers affected because of the presence of the porous medium. The *y*-component increases downward because of the increase in the velocity vectors downward (not shown here) near the moving wall.

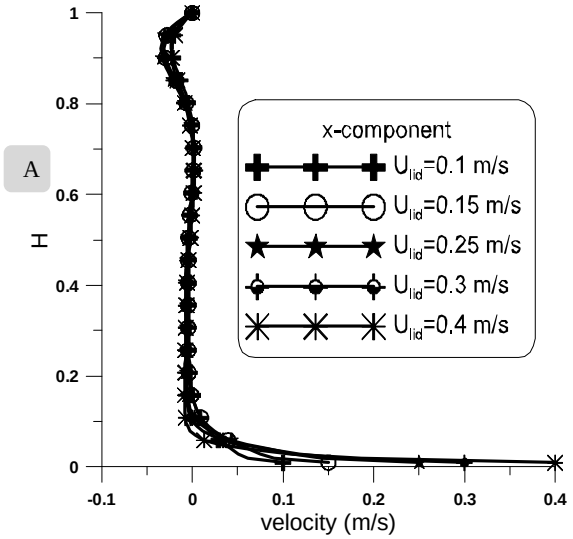

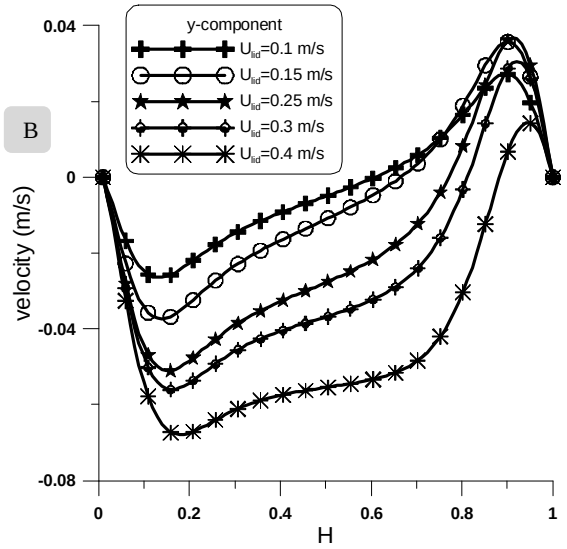

Fig. 6Velocitiesdistributions forcases (17-21)

C. Heating and cooling direction effect

Fig. 7 shows the velocity vectorand temperature contour for case (22). One big upper clockwise vortex is appeared because of the density effect due to heating. Other cases (23-25) have the same behavior and the differences are only in the directions (not shown here). In case (23) the vortex is counterclockwise and the heat is transferred from right to left with the same profile.In case (24) the vortex is clockwise and the heat is transferred from up to down. In case (25) the vortex is counterclockwise and the heat is transferred from down to up.

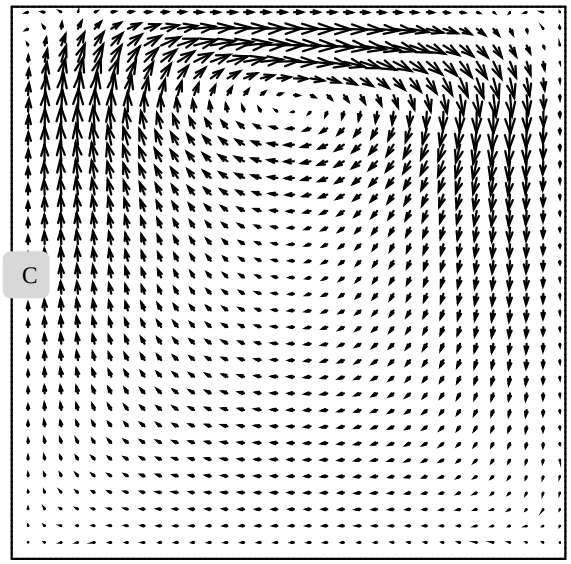

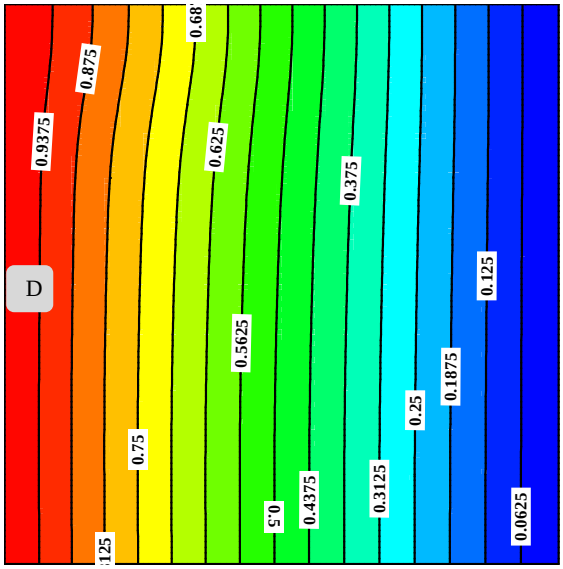

Fig. 7 Velocity vector and temperature contour for case(22).

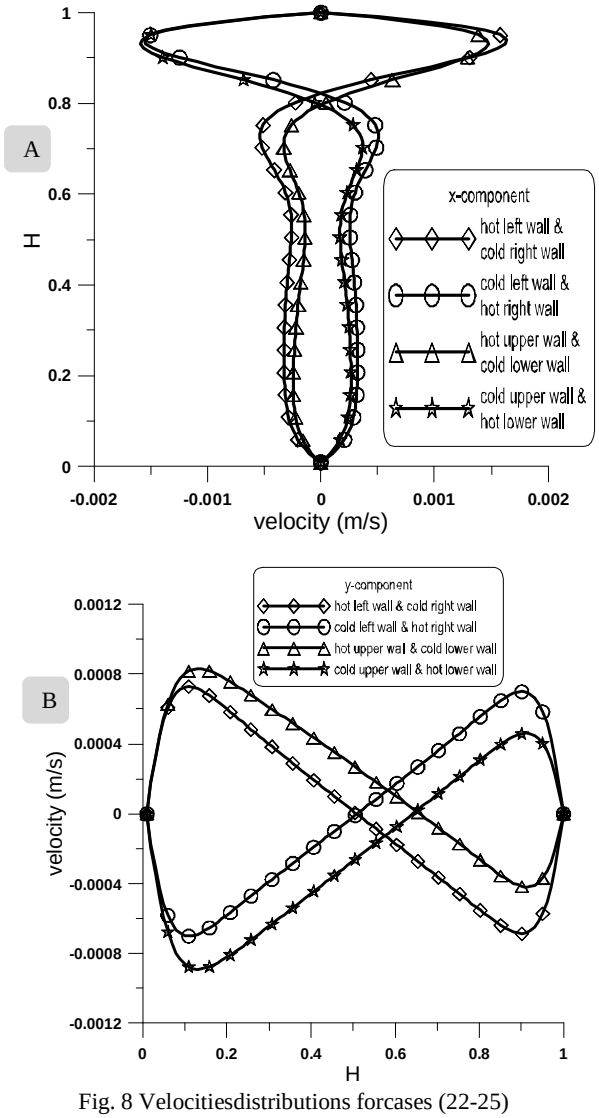

Fig. 8 Velocitiesdistributions forcases (22-25)

Fig. 8 shows the velocities distributions (*x*-component (8-A) along the box height) and (*y*-component (8-B)along the box width) for cases (22-25). A perfect symmetry is obtained.

Finally, table (3) tabulated theaverage Nusselt number $\overline{Nu}$ for all cases. The conclusions from this table are:

1- The best case is case (2) when the lower wall is moving to the right ($\overline{Nu} \approx 1.77$).
2- Cases (3, 6, 10, 16, 24, and 25) are refused because they reduce the average Nusselt number compared with no wall movement (case (22)).
3- The negative sign in case (23) refers to the opposite heat transfer direction because the hot wall is at the right.
4- The heating from up or down (cases (24 and 25)) is notdesirable because it reduces heat transfer especially when the heating from the upper wall.
5- Case (13)($\overline{Nu} \approx 1.77$) is desirable such as case (2) and the high average Nusselt number is due to the adding velocity to the single vortex from the moving walls (the upper wall moves in +*x* direction and lower one moves in -*x* direction).
6- The average Nusselt number increases as the lid velocity increases 0.1 m/s, 0.15 m/s, and 0.2 m/s (cases (17, 18, and 2)) then $\overline{Nu}$ decreases as the wall velocity increases 0.25 m/s, 0.3 m/s, and 0.4 m/s (cases (19, 20, and 21)) but all these cases have $\overline{Nu}$ more than case (22) (i.e. no movement).
7- For most of the cases the relaxation time carried by momentum = 1.1 and the relaxation time carried by energy= 0.7 and whenever the case is more complicated, the hydro and thermo relaxation times are increases such as case (15).

TABLE III
AVERAGE NUSSELT NUMBER FOR ALL CASES

Cases	$\overline{Nu}$	*Cases*	$\overline{Nu}$
Case (1)	1.654195	*Case (14)*	1.678595
Case (2)	1.766849	*Case (15)*	1.500225
Case (3)	0.042036	*Case (16)*	0.880524
Case (4)	1.494783	*Case (17)*	1.377251
Case (5)	1.502358	*Case (18)*	1.479234
Case (6)	0.071291	*Case (19)*	1.353632
Case (7)	1.458122	*Case (20)*	1.279612
Case (8)	1.476555	*Case (21)*	1.212730
Case (9)	1.431410	*Case (22)*	0.994327
Case (10)	0.180620	*Case (23)*	-0.994292
Case (11)	1.389876	*Case (24)*	0.005805
Case (12)	1.504755	*Case (25)*	0.017440
Case (13)	1.707402		

Nomenclature

c	Micro velocity vector
e	Discrete velocity
F	Total body force due to the presence of porous media
f_i	Discretized density distribution function
f_i^{eq}	Discretized equilibrium density distribution function
G	Boussinesq effect
g	Acceleration due to gravity
g_i	Discretized internal energy distribution function
g_i^{eq}	Discretized equilibrium internal energy distribution function
H	Characteristic length
j	Vertical direction opposite to that of gravity
K	Permeability
p	Pressure
T	Temperature
T_m	Average temperature
t	Time
u	Velocity vector
x	Position

Greek Symbols

β	Bulk coefficient
χ	Thermal diffusivity
Δt	Time step
ε	Porosity
ρ	Density
τ	Time relaxation
υ	Kinematic viscosity
υ_ε	Effective viscosity
ω	Weight coefficient

Non-dimensional Numbers

Nu	Nusselt number
Pr	Prandtl number
Ra	Rayleigh number
Da	Darcy number

REFERENCES

[1] EkkehardHolzbecher, "Characterisation of Heat and Mass Transfer in Porous Media," in *2000 16th IMACS World Congress*.

[2] Hakan F. Oztop, "Combined convection heat transfer in a porous lid-driven enclosure due to heater with finite length," *International Communications in Heat and Mass Transfer*, vol. *33*,pp. *772 – 779*, March 2006.

[3] WatitPakdee andPhadungsakRattanadecho, "Natural Convection in Porous Enclosure caused by Partial Heating or Cooling," in *the 20th Conference of Mechanical Engineering Network of Thailand*, 18-20 October 2006, NakhonRatchasima, Thailand.

[4] M.A.R. Sharif, "Laminar mixed convection in shallow inclined driven cavities with hot moving lid on top and cooled from bottom," *Applied Thermal Engineering*, vol.*27*,pp.*1036–1042*, March *2007*.

[5] C.Y. Wang, "The recirculating flow due to a moving lid on a cavity containing a Darcy–Brinkman medium," *AApplied Mathematical Modelling*, vol.*33*,pp.*2054–2061*, March *2009*.

[6] M.A. MohdIrwan, A. M. Fudhail, C.S. Nor Azwadi and G. Masoud, "Numerical Investigation of Incompressible Fluid Flow through Porous Media in a Lid-Driven Square Cavity," *American Journal of Applied Sciences*, vol. *7*,no. *10*, pp. *1341-1344*, *2010*.

[7] Mohamed A. Teamahand Wael M. El-Maghlany, "Numerical simulation of double-diffusive mixed convective fl ow in rectangular enclosure with insulated moving lid," *International Journal of Thermal Sciences*, vol.*49*, pp.*1625-1638*, *2010*.

[8] MohdIrwan Bin MohdAzmi, "Numerical Study of Convective Heat Transfer and Fluid Flow through Porous Media," *Masterthesis*, University Technology Malaysia, *2010*.

[9] M. R. Safaiyand H. R. Goshayeshi, "Numerical Simulation of Laminar and Turbulent Mixed Convection in Rectangular Enclosure with Hot upper Moving Wall," *Int.J.Advanced Design and Manufacturing Technology*,vol.*3*,no. *2*, *March-2010*.

[10] M. A. Waheed, G. A. Odewoleand S. O. Alagbe, "Mixed Convective Heat Transfer In Rectangular Enclosures Filled With Porous Media," *ARPN Journal of Engineering and Applied Sciences*,vol.*6*,no. *8*,pp.*47-60*,*August 2011*.

[11] Prakash Chandra and V. V. Satyamurty, "Non-Darcian and Anisotropic Effects on Free Convection in a Porous Enclosure," *Transp Porous Med*,vol.*90*,pp.*301-320*,*May2011*.

[12] IlyasKandemir and AlaattinMetin Kaya, "Molecular dynamics simulation of compressible hot/cold moving lid-driven microcavity flow," *Microfluid Nanofluid*,vol.*12*, pp.*509-520*,*2012*.

[13] Khaled Al-Salem, Hakan F. oztop, Ioan Pop and YasinVarol, "Effects of moving lid direction on MHD mixed convection in a linearly heated cavity," *International Journal of Heat and Mass Transfer*,vol. *55*, pp. *1103–1112, 2012*.

[14] Davis, D.V.,"Natural Convection of air in square cavity: a bench mark numerical solution,"*International Journal of Numerical Methods in Fluids*,vol.3, pp.249-264, 1983.

[15] Nithiarasu, P., Seetharamu, K.N. and Sundarajan,T.,"Natural convective heat transfer in a fluid saturated variable porosity medium,"*Int. J. Heat Transfer*. Vol. 40, no. 16, pp. 3955-3967, 1997.

[16] Seta, T., Takegoshi, E. and Okui, K.,"Lattice Boltzmann simulation of natural convection in porous media,"*Mathematics and Computers in Simulation*, vol.72, pp.195-200, 2006.